

Validation of MODIS aerosol optical depth retrieval over land

D. A. Chu¹, Y. J. Kaufman², C. Ichoku¹, L. A. Remer², D. Tanre³, and B. N Holben⁴

¹ Science Systems and Applications Inc., NASA/Goddard Space Flight Center, code 913, Greenbelt, MD 20771, USA. achu@climate.gsfc.nasa.gov

² Laboratory for Atmospheres, NASA/Goddard Space Flight Center, code 913, Greenbelt, MD 20771, USA.

³ Laboratoire d'Optique Atmosphérique, Centre National de la Recherche Scientifique et Université des Sciences et Technologies de Lille, Villeneuve d'Ascq, France.

⁴ Laboratory for Terrestrial Physics, NASA/Goddard Space Flight Center, code 923, Greenbelt, MD 20771, USA.

Submitted to *Geophys. Res. Lett.*

March 2001

Abstract

Aerosol optical depths are derived operationally for the first time over land in the visible wavelengths by MODIS (Moderate Resolution Imaging Spectroradiometer) onboard the EOS-Terra spacecraft. More than 300 Sun photometer data points from more than 30 AERONET (Aerosol Robotic Network) sites globally were used in validating the aerosol optical depths obtained during July - September 2000. Excellent agreement is found with retrieval errors within $\Delta\tau = \pm 0.05 \pm 0.20\tau$, as predicted, over (partially) vegetated surfaces, consistent with pre-launch theoretical analysis and aircraft field experiments. In coastal and semi-arid regions larger errors are caused predominantly by the uncertainty in evaluating the surface reflectance. The excellent fit was achieved despite the ongoing improvements in instrument characterization and calibration. This results show that MODIS-derived aerosol optical depths can be used quantitatively in many applications with cautions for residual clouds, snow/ice, and water contamination.

Introduction

The Application of satellite data to derive the distribution and properties of global aerosol is advancing dramatically in the last few years (see review by *King et al.* [1999]). One of the main advancements is the systematic derivation of aerosol over land from the MODIS (Moderate Resolution Imaging Spectroradiometer) sensor onboard EOS-Terra platform, launched into a Sun synchronous orbit (10:30 AM equator crossing time) on December 18, 1999. The validation of MODIS aerosol data product is the subject of this paper. After 3 months of adjusting orbital altitude and outgasing, on February 24 2000, MODIS began to acquire measurements with thirty-six spectral bands (0.41 - 14 μm) at three different spatial resolutions (250m, 500m and 1km)

[Salomonson *et al.*, 1989]. With a wide scan angle $\sim 110^\circ$ (or a swath width of 2,330 km), MODIS is able to produce a nearly global image everyday.

The retrieval of aerosol optical depth over land employs primarily three spectral channels centered at 0.47, 0.66, and 2.1 μm at 500m resolution. The measurements at 2.1 μm provide estimated surface reflectance at 0.47 and 0.66 μm ($\rho_{0.47\mu\text{m}}/\rho_{2.1\mu\text{m}} = 0.25$ and $\rho_{0.66\mu\text{m}}/\rho_{2.1\mu\text{m}} = 0.5$) [Kaufman *et al.*, 1997b]. Cloud-free dark pixels are selected and the corresponding radiances are averaged using a 10-40 percentile in a 10 km \times 10 km box after cloud screening by the MODIS cloud mask [Ackerman *et al.*, 1998]. More detailed illustrations of the algorithm and dynamic aerosol models for use in retrieving aerosol optical depth can be found in Kaufman *et al.* [1997a].

The β -version (partially verified but not science quality data) MODIS level 2 aerosol product was released starting on day 233 (August 20, 2000), approximately 6 months after the opening of the MODIS sensor door. Continuous updates in level 1 calibration are made throughout the period since launch, while the MODIS aerosol land algorithm remains unchanged. The improvements of aerosol retrieval over time can be attributed to improvements in the instrument calibration and in the cloud-masking algorithm.

MODIS aerosol retrievals over land are limited to the dark surfaces. Figure 1 displays the frequency map of aerosol retrieval over land between July and September 2000. Except arid and snow/ice covered regions (e.g., Antarctic continent and Greenland), aerosol retrievals successfully cover 70% of the land. Because of missing data, the color code, though varying from region to region, does not necessarily reflect the percentage of retrievals. At high latitude, more retrievals are seen because of the overlapping of satellite orbits. The MODIS aerosol land algorithm works in

tandem with aerosol ocean algorithm [Tanré *et al.*, 1997], which is validated in an accompanying paper [Remer *et al.*, 2001].

Validation approach

In order to take into account both spatial and temporal variabilities of aerosol distribution (e.g., the linkage with meteorological wind field) and also to reduce cloud contamination, MODIS retrievals and ground-based Sun photometer observations need to be co-located in space and time. In doing so, a threshold of data availability of 20% or greater is applied. In the other words, we require at least 2 (out of 5) AERONET data points nominally in a 15-min interval within ± 30 min of MODIS overpasses and at least 5 (out of 25) MODIS retrievals in a square box of $50 \text{ km} \times 50 \text{ km}$ centered at AERONET sites. The means of the co-located spatial (level 2 MODIS retrievals) and temporal (AERONET measurements) ensemble are then used in linear regression analysis and in calculating the root mean square errors. The AERONET version 1.5 data set has been integrated into a daily aerosol validation process combining with MODIS aerosol retrievals. The details about the methodology are described by Ichoku *et al.* [2001].

Aerosol Optical Depth

The global comparison between MODIS and AERONET measurements shows correlations of 0.91 and 0.85 at 0.47 and 0.66 μm wavelength, respectively, with slopes equal to 0.86 and intercepts 0.02-0.06 (see Figure 2). More than 300 points representing more than 30 Sun photometer sites meet our match-up requirements during the period of July-September 2000. Small islands (such as Bermuda, Barbados, Maldives, Cape Verde, Hawaii, etc.) and a floating platform (COVE) are considered to be ocean sites and thus are excluded. Venice and El Arenocillo excluded in the validation will be discussed later in a specific section. The slope deviating from 1

represents the systematic bias in MODIS retrievals, often attributable to the aerosol model assumptions (deviation of 0-10%) or instrument calibration (deviation of 2-5%). The deviation of the intercept from 0 is associated with errors in surface reflectance estimate. The uncertainty in surface reflectance has larger impact on low optical depth whereas the assumption of aerosol model is more sensitive to high optical depth. In the regions where pre-launch field experiments took place, we will examine the results in more detail by taking advantage of better understanding of the surface uncertainties as well as aerosol properties in those regions.

Continental In-land Region

Shown in Figures 3(a) and (b) are the comparisons between MODIS-derived aerosol optical depth and AERONET direct Sun observations [Holben *et al.*, 1998] in central US and in Brazil during the period of July - September, respectively, with dominant urban/industrial and biomass burning aerosols. These are the regions where the pre-launch SCAR-A (Sulfate, Clouds, And Radiation-Atlantic) and SCAR-B (Smoke, Clouds, And Radiation - Brazil) experiments took place. The small intercepts resulting from linear regression suggests vegetated surfaces, such as evergreen, deciduous, mixed forests, and cropland, which are expected to give the best fit to the empirical relationship [Kaufman *et al.*, 1997b]. For biomass burning aerosol in Brazil, larger deviations between MODIS and Sun photometer values are found at 0.66 μm (slope = 0.86) as compared to those at 0.47 μm , caused by overestimate of the single scattering albedo ($\omega_0 = 0.90$) [Remer *et al.*, 1998a]. According to a sensitivity study [Chu *et al.*, 1998] using MAS (MODIS Airborne Simulator) measurements acquired in SCAR-B, the single scattering albedo of 0.89 would result in a better fit. The poorer fit at 0.66 μm could be also attributed to the calibration drift

found in AERONET Sun photometer observations [*Smirnov et al.*, private communication], or the uncertainty in particle size.

The MODIS retrievals over a region with industrial/urban aerosol, or biomass burning aerosol, are based on dynamic aerosol models derived from field measurements of regional pollution in the Eastern United States (i.e., SCAR-A) and in Brazil (i.e., SCAR-B). It is shown that from Figure 3(c) the MODIS-derived aerosol optical depths over Europe resulted in similar slopes and intercepts as in the United States. Thus it implies that the differences, if any, in aerosol particle size and chemical composition between European and US pollution are small enough not to affect the retrieval. For biomass burning aerosol, the smaller slope resulted from African biomass burning (see Figure 3(d)) indicates that more soot particles (with a smaller single scattering albedo) are being emitted into the atmosphere in Africa as opposed to South America, which is in agreement with single scattering albedo retrieval by *Dubovik et al.* [2000].

Continental Coastal Zone

In the coastal area, surface inhomogeneity or sub-pixel water contamination plays a larger role than we anticipated. We examined five AERONET sites: NASA Goddard Space Flight Center, Maryland Science Center, Wallops, Venice, and El Arenosillo. Figures 4(a) and (b) display the results of coastal zones in the Europe and in the United States, respectively. Large intercepts are seen at Venice and El Arenosillo, whereas smaller intercepts are found at US coastal sites during the period being examined (July - September). The reason of causing large intercepts at Venice and El Arenosillo is not known. However, the smaller intercept of US coastal sites is in contrast to earlier results from the spring season data with larger intercepts. The spring data were closely correlated with standing water from frequent rain events, while in July-September period it was

usually dry. Some improvements planned to better handle sub-pixel-standing water will be implemented in later versions of the MODIS aerosol algorithm.

Spectral Dependence of Aerosol Optical Depth

The most common way to determine aerosols either dominated by fine or coarse mode particles is using the Angstrom coefficient. For the MODIS aerosol retrievals over land, Angstrom coefficient is calculated based upon the aerosol optical depths retrieved at 0.47 and 0.66 μm wavelengths, expressed as follows

$$\alpha = \ln(\tau_{0.47 \mu\text{m}} / \tau_{0.66 \mu\text{m}}) / \ln(0.66 / 0.47)$$

where $\tau_{0.47 \mu\text{m}}$ and $\tau_{0.66 \mu\text{m}}$ represent MODIS-derived aerosol optical depths at 0.47 and 0.66 μm wavelength, respectively. As shown in Figure 2, the MODIS-derived aerosol optical depths at 0.66 μm show more scattered distribution than that at 0.47 μm wavelength. In turn, it results in greater variability in Angstrom coefficients derived from MODIS retrievals as compared to those from AERONET observations. For a meaningful comparison, a scatter plot of the Angstrom coefficients obtained from both MODIS and AERONET is displayed for $\tau_{0.66 \mu\text{m}} > 0.2$ (see Figure 5). The improvement in the fitting of Angstrom coefficients is seen due to the decreasing surface effect as aerosol optical depth increases. Given the 10-fold possible errors in the MODIS aerosol optical depths due to surface reflectance uncertainty of 0.02 [Kaufman *et al.*, 1997b], the threshold of $\tau_{0.66 \mu\text{m}} > 0.2$ would be most appropriate for use in comparison of Angstrom coefficients. Other factors that are also sensitive to Angstrom coefficient are the uncertainties of aerosol properties, for example, the single scattering albedo as discussed previously.

Aerosol Global Distribution

The global distributions of the monthly averaged aerosol optical depth and Angstrom coefficient over land are shown in Figure 6 (a) and (b), respectively, for September 2000. The MODIS level 3 daily products at $1^\circ \times 1^\circ$ grid size were used in producing the global image. We select the month of September because of the more complete global measurements acquired in that month than in July or August. From Figure 6(a), we can clearly see the dry-season biomass burnings in African and South America, and air pollution in Europe and China. The corresponding Angstrom coefficients for September are shown in Figure 6(b), which closely correlates with distribution of aerosols—fine-mode urban/industrial and biomass burning aerosols, coarse-mode dust, and mixture of the two. Also superimposed on the images are North America regional monthly mean showing smoke plumes caused by wild fires in the US western states (Montana, Idaho, Wyoming) in August transported to the east.

Discussions and Concluding Remarks

The MODIS aerosol retrievals over land are meeting the expectations with unprecedented accuracy (errors within $\Delta\tau = \pm 0.05 \pm 0.20\tau$). With the improvements in instrument calibration, we expect the quality of the aerosol product will continue to improve with time. However, several sources of error remain to be solved, such as the sub-pixel clouds, snow/ice, and water contamination, uncertainties in heterogeneous surface reflectance, and aerosol properties beyond the scope of assumptions of dynamic aerosol models. The dust outbreak and air pollution in China is one of the good examples for testing the surface reflectance relationship and dynamic aerosol models. The ACE-Asia field campaign planned to take place in March - May 2001 will provide important insight of understanding aerosol properties in that region. Because of successful applications based upon SCAR-A and SCAR-B experiments [Kaufman *et al.*, 1997a; Chu *et al.*,

1998], we will continue to refine the MODIS aerosol algorithm by incorporating information from all available sources.

Acknowledgements

The authors would like to thank the Goddard DAAC and MODIS software development and support team for processing MODIS level 1, level 2, and level 3 data, and AERONET PIs for collecting the aerosol observations around the world.

Reference

- Ackerman, S. A., K. I. Strabala, W. P. Menzel et al., Discriminating clear-sky from clouds with MODIS, *J. Geophys. Res.*, 103, 32,141-32,158, 1998.
- Chu, D. A., Y. J. Kaufman, L. A. Remer, Remote sensing of smoke from MODIS airborne simulator during SCAR-B experiment, *J. Geophys. Res.*, 103, 31,979-31,987, 1998.
- Dubovik, O, A. Smirnov et al., Accuracy assessments of aerosol properties retrieved from AERONET Sun and sky-radiance measurements, *J. Geophys. Res.*, in press, 2000.
- Holben, B. N., T. F. Eck, I. Slutsker et al., AERONET-A federated instrument network and data archive for aerosol characterization, *Rem. Sens. Enviro.*, 66, 1-16, 1998.
- Ichoku, C., D. A. Chu et al., A spatial-temporal approach for the validation of MODIS aerosol and water vapor products, in preparation to submit to *Geophys. Res. Let.*, 2001
- Kaufman, Y. J., D. Tanre, L. A. Remer et al., Operational remote sensing of tropospheric aerosol over the land from EOS-MODIS, *J. Geophys. Res.*, 102, 17,051-17,061, 1997a.
- Kaufman, Y. J. et al., The MODIS 2.1 μm channel-Correlation with visible reflectance for use in remote sensing of aerosol, *IEEE Trans. Geosci. Remote Sens.*, 35, 5, 1286-1298, 1997b.

- King, M. D., Y. J. Kaufman, D. Tanré, and T. Nakajima, Remote sensing of tropospheric aerosols from space: past, present and future. *Bull. of Meteor. Soc.*, **80**, 2,229-2,259, 1999.
- Remer, L. A. et al., Tropical biomass burning smoke aerosol size distribution model. *J. Geophys. Res.*, 31,879-31,892, 1998.
- Remer, L. A. and Y. J. Kaufman, Dynamical aerosol model: Urban/industrial aerosol, *J. Geophys. Res.*, 103, 13,859-13,871, 1998b.
- Remer, L. A. et al., Validation of MODIS Aerosol Retrieval Over Ocean, submitted to *Geophys. Res. Let.*, 2001.
- Salomonson, V. et al., MODIS Advanced facility instrument for studies of the earth as a system. *IEEE Transactions on Geoscience and Remote Sensing*, 27(2), 145-153, 1989.
- Tanré, D. et al., Remote sensing of aerosol over oceans from EOS-MODIS, *J. Geophys. Res.*, **102**, 16,971-16,988, 1997.

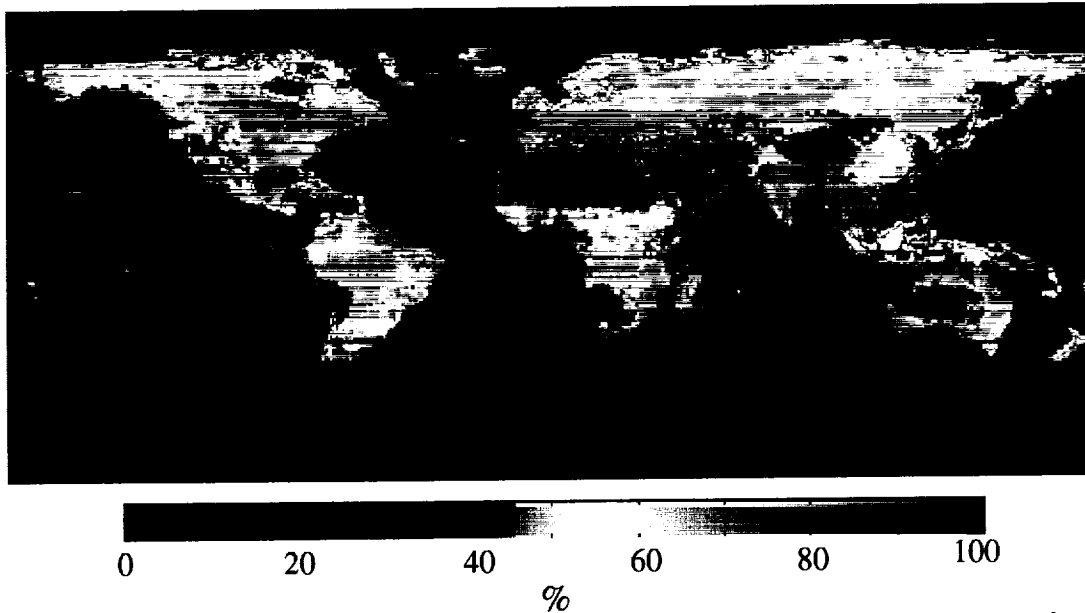
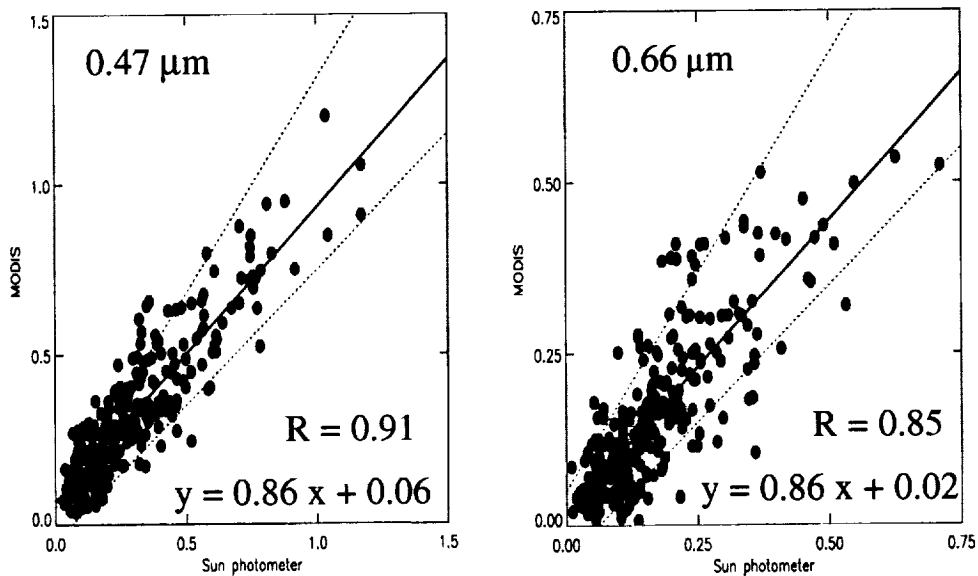


Figure 1. Frequency map of MODIS aerosol retrievals over land between July and September 2000. The frequency is derived using MODIS level 3 daily product in $1^\circ \times 1^\circ$ resolution for number of aerosol retrievals accumulated in each $1^\circ \times 1^\circ$ grid box between July and September and divided by number of calendar days instead of the number of data days available in that period.



Total points = 315; excluding Venice and El Arenosillo sites

Figure 2. Global comparison of aerosol optical depth from MODIS measurements and AERONET direct Sun photometer observations at 0.47 and 0.66 μm wavelength. This comparison includes 315 points from more than 30 AERONET Sun photometers but excludes two Venice and El Arenosillo sites.

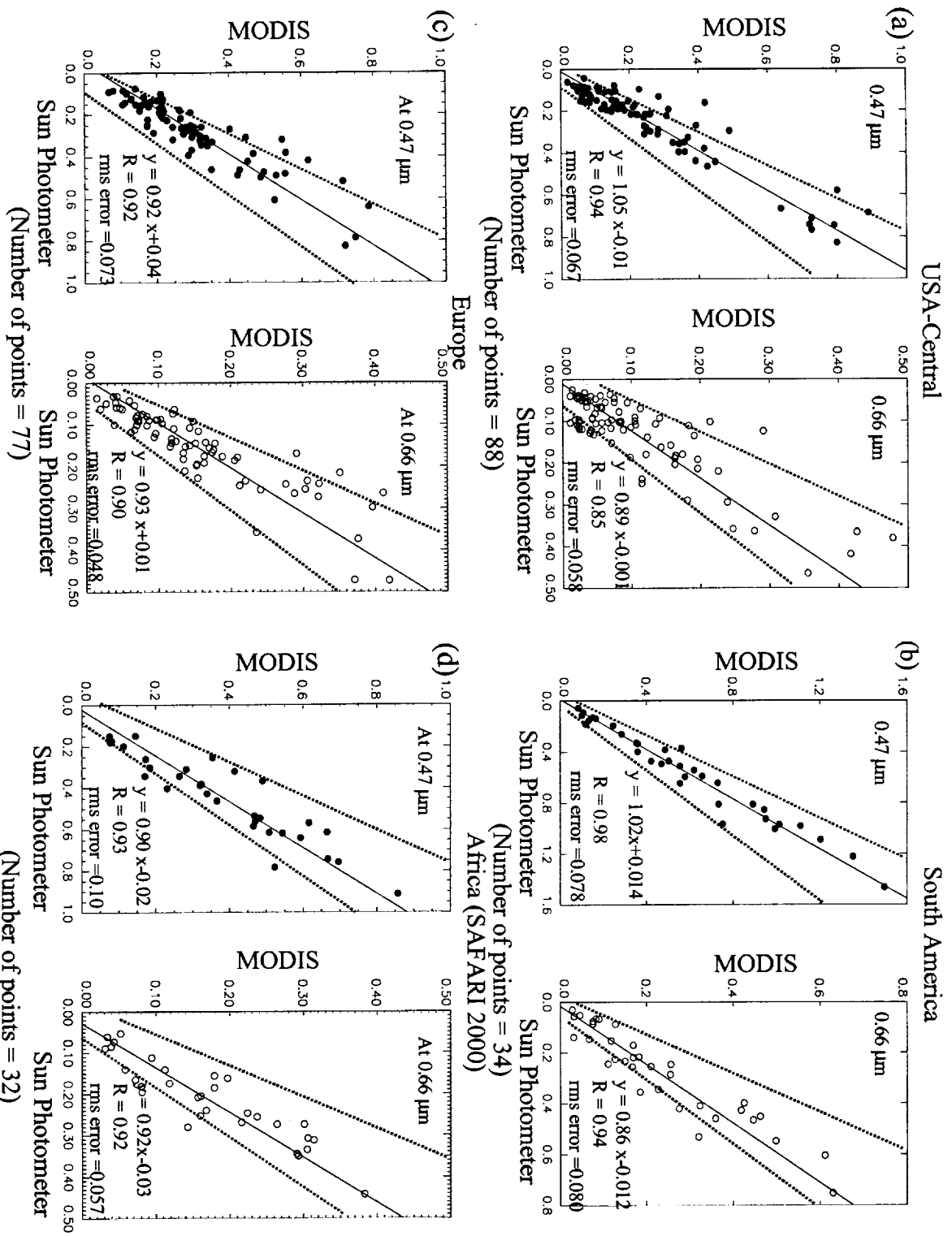


Figure 3. Regional comparison of aerosol optical depth from MODIS measurements and AERONET direct Sun photometer observations at 0.47 and 0.66 μm wavelength in continental inland regions: (a) USA central regions, (b) South America, (c) Europe, and (d) Africa.

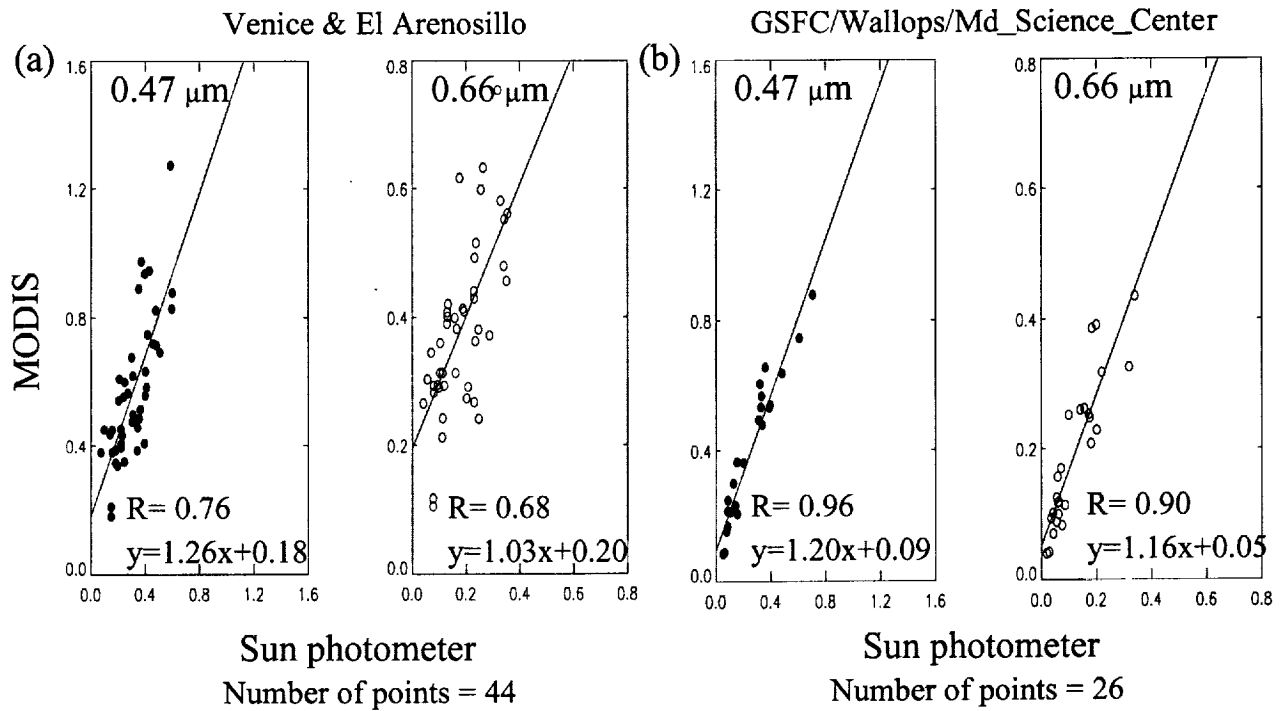


Figure 4. Regional comparison of aerosol optical depth from MODIS measurements and AERONET direct Sun photometer observations at 0.47 and 0.66 μm wavelength in continental coastal zones: (a) Venice and El Arenosillo and (b) NASA Goddard Space Flight Center, Wallops Island, and Maryland Science Center. They are grouped together for similar characteristics of aerosol retrievals.

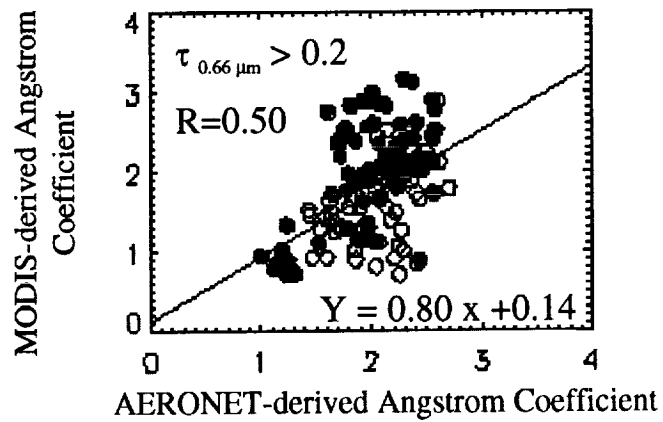


Figure 5. Comparisons of MODIS and AERONET derived Angstrom coefficients with varying thresholds of the MODIS aerosol optical depths derived at 0.66 μm wavelength (red : biomass-burning aerosol; blue: industrial/urban aerosol; green : mixed aerosol with dust particle; white: biomass-burning or industrial/urban aerosols outside the regions as discussed in Figure 3).

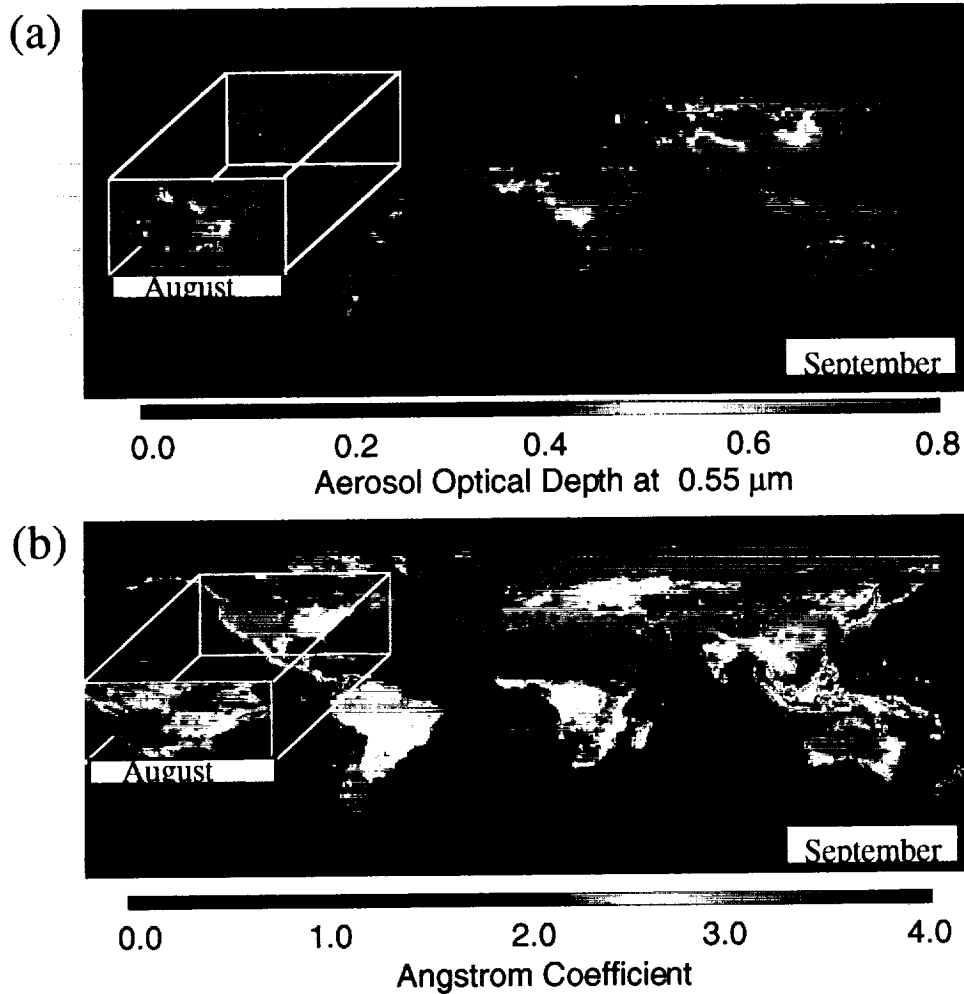


Figure 6. Monthly mean of aerosol optical depths and Angstrom coefficients retrieved from MODIS for September 2000. The monthly mean of aerosol optical depth for August is superimposed to the September image to show the transported smoke plume caused by wild fires in US western states.

Figure Captions

- Figure 1. Frequency map of MODIS aerosol retrievals over land between July and September 2000. The frequency is derived using MODIS level 3 daily product in $1^\circ \times 1^\circ$ resolution for number of aerosol retrievals accumulated in each $1^\circ \times 1^\circ$ grid box between July and September and divided by number of calendar days instead of the number of data days available in that period.
- Figure 2. Global comparison of aerosol optical depth from MODIS measurements and AERONET direct Sun photometer observations at 0.47 and 0.66 μm wavelength. This comparison includes 315 points from more than 30 AERONET Sun photometers but excludes two Venice and El Arenosillo sites.
- Figure 3. Regional comparison of aerosol optical depth from MODIS measurements and AERONET direct Sun photometer observations at 0.47 and 0.66 μm wavelength in continental inland regions: (a) USA central regions, (b) South America, (c) Europe, and (d) Africa.
- Figure 4. Regional comparison of aerosol optical depth from MODIS measurements and AERONET direct Sun photometer observations at 0.47 and 0.66 μm wavelength in continental coastal zones: (a) Venice and El Arenosillo and (b) NASA Goddard Space Flight Center, Wallops Island, and Maryland Science Center. They are grouped together for similar characteristics of aerosol retrievals.
- Figure 5. Comparisons of MODIS and AERONET derived Angstrom coefficients with varying thresholds of the MODIS aerosol optical depths derived at 0.66 μm wavelength (red : biomass-burning aerosol; blue: industrial/urban aerosol; green : mixed aerosol with dust

particle; white: biomass-burning or industrial/urban aerosols outside the regions as discussed in Figure 3).

Figure 6. Monthly mean of aerosol optical depths and Angstrom coefficients retrieved from MODIS for September 2000. The monthly mean of aerosol optical depth for August is superimposed to the September image to show the transported smoke plume caused by wild fires in US western states.